Vol 10 No 6, June 2001
1009-1963/2001/10(06)/0505-07
Chinese Physics
© 2001 Chin. Phys. Soc.
and IOP Publishing Ltd

CALCULATION OF THE FINE STRUCTURE OF OXYGEN-LIKE IONS USING THE POLARIZATION POTENTIAL FUNCTION*

Sheng Yong(盛 勇), Wang Rong(汪 蓉),
Jiang Gang(蒋 刚), and Zhu Zheng-he(朱正和)
Institute of Atomic and Molecular Physics, Sichuan University, Chengdu 610065, *China*

(Received 9 August 2000; revised manuscript received 9 January 2001)

We have calculated the forbidden transition energies and magnetic dipole transition probabilities of $2s^22p^4(^3P_1$–$^3P_2)$ and $2s^22p^4$ $(^3P_0$–$^3P_1)$ of oxygen-like isoelectronic sequences (Z=10–32) by a method of polarization potential correction. The transition energies show good agreement with experiment and are much better than the calculations in the literature. These results also illustrate that it is feasible to use the dipole expansion of the polarization potential to deal with some dynamic and non-dynamic effects in the central field approach. The relation of polarizability and cut-off radius with atomic number is discussed. We also give the fitted formula between the polarizability α_1 and atomic number Z as $\alpha_1=0.73429-9.56644\times10^{-4}Z+7.43016\times10^{-5}Z^2-2.53298\times10^{-6}Z^3+2.08306\times10^{-8}Z^4$.

Keywords: oxygen-like isoelectronic sequences, forbidden transition, polarization potential, polarizability
PACC: 3130, 3220R, 3150

I. INTRODUCTION

The astronomer's request for atomic data has always been a strong incitement for atomic spectroscopy, experimental as well as theoretical. Accurate wavelength and transition probabilities are needed for the analysis of solar and stellar spectra.[1–3] Recently there has been considerable interest in the transition energy of the fine structure of oxygen-like (O-like) ions. Because it is magnetic dipole (M_1) spectroscopic data, it is a dominant charge-state over a wide range of plasma parameters. As a result, O-like ions of low and medium Z exist in various high-temperature plasma sources.[4–6] Thus the spectra of O-like isoelectronic sequences is of fundamental importance in the research on high-temperature plasma. Another reason for studying the O-like ions is that the energy levels of O-like ions provide important information about the M_1 transition and electronic quadrupole (E_2) transition of energy shift which are important for understanding the relativistic and quantum electrodynamics effects in multi-electron systems. At the same time, the study of the O-like ions may further develop the theory of quantum mechanics and the calculation of multi-electron systems.

Much work has been carried out in theory and experiment in the last twenty years.[4–16] In the calculation of highly stripped atoms, it is worth pointing out that different methods, such as the z-expansion method (MZ), model potential method (MPM or PM), basic method (BAS), multi-configuration Dirac-Fock (MCDF) method, etc,[17] are suitable only for certain ranges of atoms. The present calculations are performed using the version GRASP2 of Grant's multi-configuration Dirac-Fock package.[18] The development of equipment and the improvement in experimental accuracy not only give theoreticians reliable data, but also bring with them new problems.

The core polarization has been used to explain the atomic structure of alkaline metals, and from the classical theory the polarizability of the core has been calculated. Temkin[19] discussed atomic polarization using full quantum mechanics. Later, many studies were carried out on the polarization of atoms and ions exposed to the external electronic field, obtaining various polarization features of some simple atoms and ions. Not so much work has been performed on the calculation of the atomic structures using the polarized orbital. However, in recent years, the calculation of the atomic structure by adding the polarization to the orbital has aroused much interest. By means of the polarization potential energy for some atoms, more information about the orbital polarization can be found.[5,20]

In this paper, starting from the orbital polarization of the core electrons, we calculate the transition energies and M_1&E_2 transition probabilities of O-like

*Project supported by the Science Foundation of China Academy of Engineering Physics (Grant No. 98020207).

isoelectronic sequences (Z=10–32) by adding the polarization potential to the orbital 2p and using the extended averaged level (EAL) procedure of the multi-configuration Dirac-Fock method. Our present results of the magnetic dipole transition energy are in excellent agreement with the experimental data.

Ⅱ. THEORETICAL METHOD

The calculations we employed are based on a fully relativistic multi-configuration Dirac-Fock self-consistent field treatment. The details of our theoretical method, the numerical procedures and the computer program have been described in Ref.[18]. The relativistic Dirac-Fock Hamiltonian is taken to be (in a.u.)

$$\hat{H} = \sum_{i=1}^{N} \hat{H}_i + \sum_{i<j}^{N} |\hat{r}_i - \hat{r}_j|^{-1}, \tag{1}$$

where all the dominant interactions of electrons are included, $\hat{H}_i$ is the relativistic Dirac-Fock Hamlitonian for the ith electron in atomic units. Using the standard notation, $\hat{H}_i$ is given by

$$\hat{H}_i = c\hat{\boldsymbol{\alpha}} \cdot \hat{\boldsymbol{P}}_i + (\beta - 1)c^2 + V_{\rm nuc}(\boldsymbol{r}), \tag{2}$$

where $V_{\rm nuc}(\boldsymbol{r})$ is the nuclear potential at $\boldsymbol{r} = \boldsymbol{r}_i$ due to the nucleus, $\hat{\boldsymbol{\alpha}}$ and β are the Dirac-Fock vector and scalar matrices, respectively, $\hat{\boldsymbol{P}}$ is the relativistic parity operator and c is the velocity of light in vacuum.

The central field Dirac orbital of a single electron is given by

$$\langle \hat{\boldsymbol{r}} | nkm \rangle = \frac{1}{r} \begin{bmatrix} P_{nk}(\boldsymbol{r}) & \chi_{km}(\hat{\boldsymbol{r}}/\boldsymbol{r}) \\ {\rm i}Q_{nk}(\boldsymbol{r}) & \chi_{-km}(\hat{\boldsymbol{r}}/\boldsymbol{r}) \end{bmatrix}, \tag{3}$$

where $P_{nk}(\boldsymbol{r})$ and $Q_{nk}(\boldsymbol{r})$ are the large and small component radial wavefunctions, respectively, and the function $\chi_{km}(\hat{\boldsymbol{r}}/\boldsymbol{r})$ is the spinor spherical harmonic.

A configuration state function (CSF), $|\gamma PJM\rangle$, of an N-electron system is formed by taking linear combinations of Slater determinants of order N constructed from orbitals (3) so as to obtain normalized eigenfunctions of the parity operator $\hat{\boldsymbol{P}}$ and the total angular momentum operators $\hat{\boldsymbol{J}}^2$ and $\hat{\boldsymbol{J}}_Z$. The atomic state function (ASF) is a linear combination of the CSF sharing common values of P, J and M. Then the energy of the atomic state Γ is $E_\Gamma^{\rm DC} = \langle \Gamma PJM | H^{\rm DC} | \Gamma PJM \rangle$.

It is impossible to involve all interactions to solve the Hamiltonian equation, as there are a great number of factors affecting each other in the highly stripped ion. In the polarization model, an additional potential on the valence electron is an important physical effect. There are two distinct parts of our procedure. In the first place, we must obtain the orbital wavefunction that describes the core electrons which, in contrast with the usual procedure, are now influenced by the adiabatic field of the valence electron. The polarized core orbitals form the basis of our polarization potential, which is used to derive the valence electron orbital in the second stage. In this paper, we employ the following optical potential $V_{\rm pol} = -\frac{\alpha_1}{r^4}(1 - {\rm e}^{-(r/r_{\rm cut})^6})$, which will be added to the Dirac-Fock equation. The symbol α_1 is the dipole polarizability. The symbol $r_{\rm cut}$ is an empirical cut-off radius parameter. We only take account of the dipole approximation and neglect high-order polarization corrections.

Ⅲ. CALCULATION RESULTS

Based on the discussion above, the present work employs the MCDF procedure with the Fermi nucleus model and takes into account the QED effect and Breit correction. It is desirable to examine the orbital polarization effect, adding the orbital polarization to 2p. After choosing configurations properly, the transition intervals, M_1 transition probabilities (A_{M_1}) of $2s^22p^4$ ($^3P_1$–$^3P_2$) and ($^3P_0$–$^3P_1$) and E_2 transition probabilities (A_{E_2}) of $2s^22p^4$ ($^3P_2$–$^3P_0$) of O-like ions are calculated. The results are given in tables 1, 2 and 3. All of the transition energy intervals are in units of kaysers.

Table 1. Comparison between theoretical (including our calculation and other authors' calculations) and experimental transition energy intervals of $2s^22p^4$ ($^3P_1$–$^3P_2$) of O-like ions (in cm^{-1}).

Z	$E^{\rm a}_{\rm exp\ t}(^3P_1$–$^3P_2)$		$E^{\rm b}_{\rm the\ o}(^3P_1$–$^3P_2)$	$E^{\rm c}_{\rm the\ o}(^3P_1$–$^3P_2)$	$E^{\rm d}_{\rm the\ o}(^3P_1$–$^3P_2)$	$\alpha_1^{\rm e}$
10	643	±1	643.5	562	643	0.72975
11	1106	±2	1104.5	1020	1107	0.72973
12	1783	±8	1783.0	1688	1783	0.72962
13	2733	±10	2731.8	2620	2733	0.72949
14	4030	±13	4029.3	3906	4028	0.72934

Table 1. (*Continued*)

Z	$E^{a}_{exp\ t}(^3P_1–^3P_2)$		$E^{b}_{the\ o}(^3P_1–^3P_2)$	$E^{c}_{the\ o}(^3P_1–^3P_2)$	$E^{d}_{the\ o}(^3P_1–^3P_2)$	α^{e}_1
15	5756	±16	5754.0	5606	5748	0.72918
16	7989	±20	7984.9	7821	7985	0.72900
17	10839	±20	10836.4	10646	10847	0.72879
18	14453	±2	14454.3	14225	14455	0.72850
19	18995	±30	18987.0	18674	18945	0.72815
20	24464	±3	24465.4	24148	24465	0.72794
21	31182	±3	31184.2	30813	31183	0.72754
22	39280	±2	39278.2	38811	39277	0.72714
23	48939	±20	48940.3	48447	48939	0.72656
24	60376	±4	60375.4	59804	60375	0.72618
25	73829	±90	73838.7	73105	73800	0.72546
26	89440	±4	89430.5	88735	89439	0.72471
27	107450	±120	107519.9	106691	107527	0.72384
28	128287	±30	128290.0	127432	128308	0.72295
29	152045	±45	152011.0	151007	152036	0.72195
30	178904	±180	178957.0	177851	178973	0.72078
31			209334.3	208160	209389	0.71977
32	243483	±100	243500.2	242180	243568	0.71874

a: Experimental transition energy intervals[7].

b: Present calculation of the transition energy intervals with orbital polarization.

c: Present calculation of the transition energy intervals without orbital polarization.

d: Other calculation energy intervals[9].

e: For all the orbital polarizabilities listed, the cut-off radius is fixed to be 0.73.

Table 2. Comparison between theoretical (including our calculation and other authors' calculations) and experimental transition energy intervals of $2s^22p^4$ ($^3P_0–^3P_1$) of O-like ions (in cm^{-1}).

Z	$E^{a}_{exp\ t}(^3P_0–^3P_1)$		$E^{b}_{the\ o}(^3P_0–^3P_1)$	$E^{c}_{the\ o}(^3P_0–^3P_1)$	$E^{d}_{the\ o}(^3P_0–^3P_1)$	r^{e}_{cut}	α^{f}_1
10	278	±4	278	278	278	0.73000	0.72975
11	470	±6	469	469	469	0.73023	0.72973
12	739	±8	741	738	738	0.73030	0.72962
13	1096	±10	1098	1094	1094	0.73036	0.72949
14	1535	±13	1536	1540	1540	0.73030	0.72934
15	2073	±16	2076	2069	2069	0.73020	0.72918
16	2642	±20	2650	2663	2663	0.72960	0.72900
17	3277	±20	3274	3280	3280	0.72850	0.72879
18	3819	±30	3825	3852	3852	0.72530	0.72850
19	4253	±30	4231	4279	4279	0.71800	0.72815
20	4428	±35	4429	4415	4415	0.70500	0.72794
21	4135	±50	4147	4076	4076	0.68410	0.72754
22	3064	±30	3065	3032	3032	0.65740	0.72714
23	1050	±50	1046	1005	1005	0.76990	0.72656
24	–2406	±80	–2410	–2325	–2325	0.77870	0.72618
25	–7295	±90	–7292	–7295	–7295	0.78741	0.72546
26	–14131	±100	–14167	–14251	–14251	0.79941	0.72471
27	–23497	±120	–22443	–23535	–23535	0.81666	0.72384
28	–35473	±3	–35473	–35472	–35472	0.84130	0.72295
29	–50560	±160	–50569	–50374	–50374	0.87800	0.72195
30	–68653	±180	–68643	–68536	–68536	0.92440	0.72078
31			–90857	–76644	–90242	0.96100	0.71977
32	–115727	±240	–115739	–115775	–115775	1.18000	0.71874

a: Experimental transition energy intervals[7].

b: Present calculation of the transition energy intervals with orbital polarization.

c: Present calculation of the transition energy intervals without orbital polarization.

d: Other calculated energy intervals[9].

e: Cut-off radius $r_{\rm cut}$.

f: Orbital polarizability.

Table 3. Comparison between transition probability (in s^{-1}) of M_1&E_2 with and without polarization for $2s^22p^4$ ($^3P_0$–$^3P_1$), ($^3P_1$–$^3P_2$) and ($^3P_0$–$^3P_2$) of O-like ions.

Z	$M_1(^3P_2$–$^3P_1)$	$M_1(^3P_2$–$^3P_1)$	$M_1(^3P_2$–$^3P_1)$	$M_1(^3P_1$–$^3P_0)$	$M_1(^3P_1$–$^3P_0)$	$M_1(^3P_1$–$^3P_0)$	$E_2(^3P_2$–$^3P_0)$	$E_2(^3P_2$–$^3P_0)$
	Ref.[21]	Cal.(pol)	Cal.(nonpol.)	Ref.[21]	Cal.(pol.)	Cal.(nonpol.)	Cal.(pol.)	Cal.(nonpol.)
10	5.79×10^{-3}	5.954×10^{-3}	3.961×10^{-3}	1.15×10^{-3}	1.164×10^{-3}	7.648×10^{-4}	2.733×10^{-8}	1.226×10^{-8}
11	3.04×10^{-2}	3.010×10^{-2}	2.373×10^{-2}	5.58×10^{-3}	5.791×10^{-3}	4.527×10^{-3}	1.690×10^{-7}	1.171×10^{-7}
12	1.27×10^{-1}	1.256×10^{-1}	1.075×10^{-1}	2.17×10^{-2}	2.292×10^{-2}	1.953×10^{-2}	9.432×10^{-7}	7.863×10^{-7}
13	4.58×10^{-1}	4.549×10^{-1}	4.015×10^{-1}	7.10×10^{-2}	7.611×10^{-2}	6.737×10^{-2}	4.493×10^{-6}	4.072×10^{-6}
14	1.47×10^{0}	1.457×10^{0}	1.328×10^{0}	1.94×10^{-1}	2.164×10^{-1}	1.992×10^{-1}	1.860×10^{-5}	1.772×10^{-5}
15	4.28×10^{0}	4.237×10^{0}	3.918×10^{0}	4.70×10^{-1}	5.385×10^{-1}	5.075×10^{-1}	6.763×10^{-5}	6.588×10^{-5}
16	1.14×10^{1}	1.129×10^{1}	1.061×10^{1}	1.01×10^{0}	1.180×10^{0}	1.139×10^{0}	2.180×10^{-4}	2.161×10^{-4}
17	6.63×10^{1}	2.812×10^{1}	2.666×10^{1}	3.00×10^{0}	2.303×10^{0}	2.261×10^{0}	6.344×10^{-4}	6.347×10^{-4}
18	2.83×10^{1}	6.642×10^{1}	6.334×10^{1}	1.87×10^{0}	3.994×10^{0}	3.980×10^{0}	1.689×10^{-3}	1.697×10^{-3}
19	1.50×10^{2}	1.496×10^{2}	1.424×10^{2}	1.32×10^{0}	6.055×10^{0}	6.118×10^{0}	4.141×10^{-3}	4.159×10^{-3}
20	3.19×10^{2}	3.177×10^{2}	3.057×10^{2}	4.19×10^{0}	7.791×10^{0}	8.027×10^{0}	9.306×10^{-3}	9.397×10^{-3}
21	6.55×10^{2}	6.522×10^{2}	6.297×10^{2}	3.66×10^{0}	8.116×10^{0}	8.559×10^{0}	1.945×10^{-2}	1.968×10^{-2}
22	1.30×10^{3}	1.289×10^{3}	1.245×10^{3}	1.41×10^{0}	6.101×10^{0}	6.707×10^{0}	3.790×10^{-2}	3.833×10^{-2}
23	2.47×10^{3}	2.466×10^{3}	2.394×10^{3}	5.10×10^{-2}	2.433×10^{0}	2.895×10^{0}	6.894×10^{-2}	6.996×10^{-2}
24	4.58×10^{3}	4.180×10^{3}	4.446×10^{3}	1.93×10^{-1}	3.139×10^{-1}	1.839×10^{-1}	1.177×10^{-1}	1.194×10^{-1}
25	8.17×10^{3}	8.244×10^{3}	8.011×10^{3}	5.15×10^{0}	2.805×10^{-1}	1.645×10^{-1}	1.889×10^{-1}	1.917×10^{-1}
26	1.45×10^{4}	1.443×10^{4}	1.411×10^{4}	4.03×10^{1}	8.619×10^{0}	7.217×10^{0}	2.861×10^{-1}	2.907×10^{-1}
27	2.47×10^{4}	2.470×10^{4}	2.416×10^{4}	1.75×10^{2}	6.165×10^{1}	5.507×10^{1}	4.110×10^{-1}	4.178×10^{-1}
28	4.14×10^{4}	4.132×10^{4}	4.054×10^{4}	5.72×10^{2}	2.639×10^{2}	2.444×10^{2}	5.631×10^{-1}	5.725×10^{-1}
29	6.78×10^{4}	6.775×10^{4}	6.642×10^{4}	1.55×10^{3}	5.589×10^{2}	8.057×10^{2}	7.396×10^{-1}	7.518×10^{-1}
30	1.09×10^{5}	1.087×10^{5}	1.068×10^{5}	3.73×10^{3}	2.327×10^{3}	2.214×10^{3}	9.364×10^{-1}	9.516×10^{-1}
31	1.72×10^{5}	1.715×10^{5}	1.687×10^{5}	8.11×10^{3}	5.550×10^{3}	5.334×10^{3}	1.149×10^{0}	1.167×10^{0}
32	2.66×10^{5}	2.659×10^{5}	2.619×10^{5}	1.64×10^{4}	1.202×10^{4}	1.162×10^{4}	1.373×10^{0}	1.393×10^{0}

1. Fig.1 shows that the polarizability α_1 decreases with the atomic number Z. First, the curve's tendency is reasonable. Since the force with which the atomic nucleus attracts core electrons increases with Z, so the larger the atomic number, the smaller the polarizability. The curve shows that α_1 decreases slowly within the range of Z from 10 to 21, but decreases rapidly in the range of Z=22–32. The curve is nearly straight in the high-Z end. The polarization parameters we have chosen, according to the corresponding transition energy, are fitted by a formula that illustrates the relation between the polarizability α_1 and atomic number Z

$$\alpha_1 = 0.73429 - 9.56644\times10^{-4}Z + 7.43016\times10^{-5}Z^2 - 2.53298\times10^{-6}Z^3 + 2.08306\times10^{-8}Z^4.$$

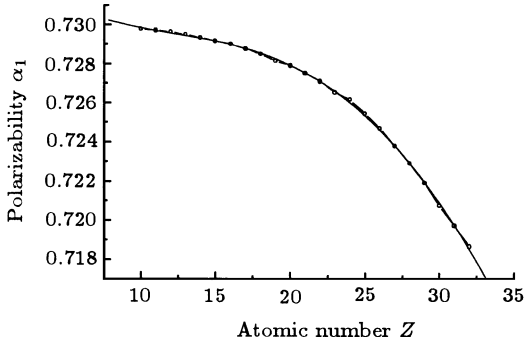


Fig.1. Atomic number Z versus polarizability α_1 curve.

The M_1 transition energies of $2s^22p^4(^3P_1$–$^3P_2)$ and ($^3P_0$–$^3P_1$) of the O-like ion, which we have calculated with the polarizability α_1 given above, agree well with experiment, so the polarization parameters chosen are reasonable in the range where the atomic number Z is from 10 to 32. From the fitted formula,

it is obvious that the transition energies are very sensitive to the polarizability, as the accuracy of polarizability reaches 10^{-5} orders.

Generally speaking, it is considered that the atomic orbital polarization is only caused by the Coulomb interaction of valence electrons. But we think that, in addition to the Coulomb repulsion, there are other reasons to make the orbital polarize. Under the central field approach, the core with $(N-1)$ electrons has a spherical symmetry. However, when the $2p^4$ in the configuration $1s^2 2s^2 2p^4$ loses an electron and change into $2p^3$, the $2p^3$ will lose its spherical symmetry. Then the 2p orbital will show polarization under the classical conditions. On the other hand, according to the Coulomb repulsion rule, it is impossible for the valence electron to stay with other electrons in the same position or even in a small volume. This forms a so-called Coulomb hole. The Coulomb hole effect will destroy the symmetrical properties of the distribution of the core electrons, so orbital polarization of the core electrons occurs.[5] The Fermi hole effect is similar to the Coulomb hole effect. As may be inferred from this, various correlation effects form the polarization.

2. The calculated M_1 transition energies of $2s^2 2p^4$ ($^3P_1$–$^3P_2$) of O-like ions with the correction of polarization potential are identical with the corresponding experimental values of curve 1 in Fig.2. Curves 4 and 5 represent the positive and negative experimental errors, respectively. Curve 2 shows the calculation error of Ref.[21]. All of our calculated energies are within the range of experimental error, and our values are better than those given in Ref.[9]. Since the absolute value of experimental error rises with the atomic number, curve 3 in Fig.2 does not go smoothly with the error variation of experimental values. The reasons that curve 3 rises gradually are that, on one hand, the transition energies of the $E^{\rm c}_{\rm theo}$ and $E^{\rm a}_{\rm exp\ t}$ of $2s^2 2p^4$($^3P_1$–$^3P_2$) increase, and on the other hand the screening is larger than the real state without considering polarization. The difference between $E^{\rm c}_{\rm the\ o}$ and $E^{\rm a}_{\rm exp\ t}$ will be larger with Z by high power. From table 1, the calculated value at Z=27 means that the real transition energy should be the $E^{\rm a}_{\rm exp\ t}$ plus a negative error value from 0 to $+120{\rm cm}^{-1}$, not from 0 to $-120{\rm cm}^{-1}$. The situations are similar at Z=30 and 32.

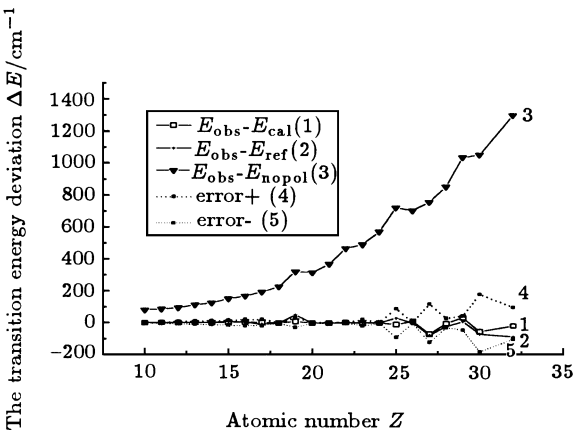


Fig.2. Atomic number Z versus transition energy deviation E curves.

3. In order to study the regularity of cut-off radius parameter, we choose different values for different atomic number Z, while every element has the corresponding polarizability given in the last column of table 1 (see Fig.3). On choosing suitable $r_{\rm cut}$, the transition energies of $2s^2 2p^4$ ($^3P_0$–$^3P_1$) of O-like isoelectronic sequence are in good agreement with experimental values. This shows that it is feasible to change the peak point of polarization potential function to obtain rational values.

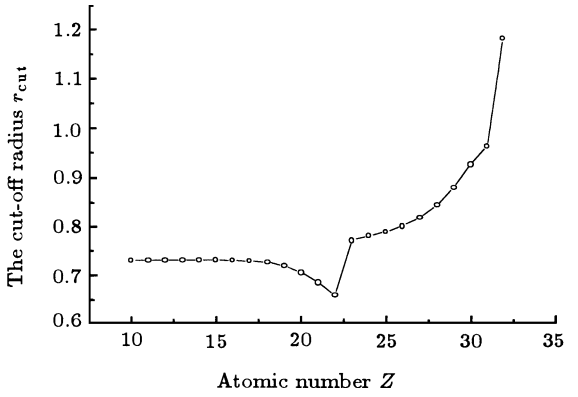


Fig.3. Atomic number Z versus cut-off radius $r_{\rm cut}$.

The $r_{\rm cut}$ decreases slowly with Z from 10 to 23. The energy interval $2s^2 2p^4$ ($^3P_0$–$^3P_1$) (see table 2) changes sign at Z=24, and from then on its size as well as the intensity of the forbidden transition begins to increase rapidly (see Fig.4). But we cannot find a suitable reason to explain why the cut-off radius begins to increase with Z after Z=24. We note that the relation between $r_{\rm cut}$ and Z has almost nothing to do with the polarizability in the range of table 1. Moreover, the results calculated without the polarization potential have a similar diagram. From Z=19 upward, the

deviations $E^{a}_{exp\ t}$–$E^{c}_{the\ o}(^3P_0$–$^3P_1)$ increase gradually, and at Z=32 the deviation is as high as about 12.8%. This shows that the polarization potential correction is very important.

4. The M_1 transition probabilities (A_{M_1}) increase slowly in the range Z=10–24, and rapidly at Z=25–32 in Fig.5, which are closer to the values in Ref.[21] than the A_{M_1} without polarization potential. As the energy interval changes sign, the A_{M_1} of ($^3P_1$–$^3P_0$) decreases suddenly at Z=24, instead of 23 as given in Ref.[21]. Not only the r_{cut} changes, but also the transition probability changes markedly at Z=24, and the latter increases very rapidly with Z from 25 to 32. As A_{M_1} is about five orders larger than A_{E_2}, the electronic quadrupole transitions, which have a similar relation with A_{M_1}, are hardly observed in the solar and plasma spectra. In this work, only dipole approximation is taken account of, and there is little difference between polarization and nonpolarization.

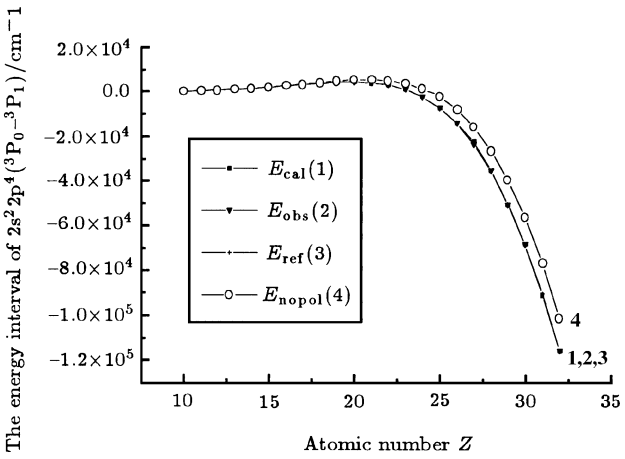


Fig.4. Transition energy intervals $2s^22p^4$ ($^3P_0$–$^3P_1$) versus Z.

5. In accurate calculations of atomic fine structure, dynamic and nondynamic correlation effects, which involve ground-state correlation, Coster-Kronig-type fluctuation, QED correction, Coulomb hole effect, and Fermi hole effect etc., are the most important aspects. It is very difficult to estimate some of the effects accurately, especially the Coulomb effect. There are few reports on the Coulomb hole effect in the calculation of atomic structure. From another point of view, all of these effects can finally be expressed as an additional potential acting on the excited electron,[5,7] so we try to use the form of polarization potential to express this kind of potential. Here we have supposed that the potential has the form of a central field pointing to the nucleus. Because the chosen r_{cut} is an empirical parameter, the polarizability α_1 fitted with experimental values is not the only parameter chosen. With a little variation of r_{cut}, α_1 will vary a little correspondingly. Even so, we might think that whatever value r_{cut} takes in the range estimated, the physical nature of the relation between corresponding α_1 and atomic number Z is true. On the other hand, while α_1 varies, the polarization potential will change, which is the correction to all related effects of an atom rather than only to the antisymmetry of the geometry. All of our results show that it is feasible to use a central field potential to express approximately all of the effects mentioned above. It is right, at least, in our calculations.

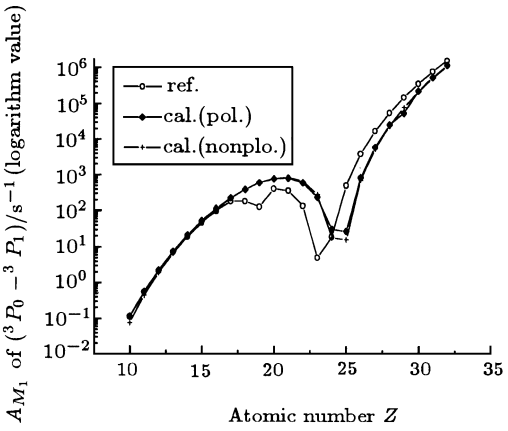


Fig.5. M_1transition probability of ($^3P_0$–$^3P_1$) versus Z.

V. CONCLUSION

The above analysis of the forbidden transition of the O-like isoelectronic sequence demonstrates the effectiveness of the polarization potential function method, which is based on the relativistic multiconfiguration Dirac-Fock treatment method. By using the form of the first-order polarization potential, we have proved that it is feasible to sum all of the effects, to which we have not given enough estimation and have ignored in our calculation procedure, into a central field potential to calculate the M_1 transition energies and probabilities of $2s^22p^4$ ($^3P_1$–$^3P_2$) and ($^3P_0$–$^3P_1$) of O-like ions. For the empirical method using the polarization potential energy, the results obtained are in good agreement with experiment.

ACKNOWLEDGMENTS

Z H Zhu would like to thank Professor I P Grant and Dr P Marketos for supplying the latest version GRASP2 of the original MCDF packuge.

References

[1] Dubau J and Volonte S 1980 *Rep. Prog. Phys.* **43** 199

[2] Fawcett B C 1981 *Phys. Scr.* **24** 663

[3] Martinson I 1989 *Rep. Prog. Phys.* **52** 157

[4] Slater J C 1986 *Quantum Theory of Atomic Structure* (New York: McGraw-Hill) Vol **1** D C Washington p68

[5] Li X D, Zhu Z H and Tan M L 2000 *Chin. Phys.* **9** 13

[6] Fawcett B C 1991 *At. Data. Nucl. Data Table* **48** 25

[7] Edlen B 1982 *Phys. Scr.* **26** 71

[8] Kaufman V, Sugar J and Cooper D 1982 *Phys. Scr.* **25** 623

[9] Edlen B 1983 *Phys. Scr.* **28** 51

[10] Hinnov E, Suckewer S, Cohen S and Sato K 1982 *Phys. Rev.* A **25** 2293

[11] Baluja K L and Zeippen G J 1988 *J. Phys.* B **21** 1455

[12] Gaigalas G, Kaniausks J, Kicisielius R, Merkelis G and Vikas M J 1994 *Phys. Scr.* **49**(2) 135

[13] Wang W J, Jiang R B and Wang X D 1996 *Nucl. Sci. Tech.* **7**(3) 154

[14] Galavis M E, Mendoza C and Zeippen C J 1997 *Astron. Astrophys. Supppl. Ser.* **123** 159

[15] Fischer C F, He X and Jonsson P 1998 *Eur. Phys. J.* **4** (3) 285

[16] Mclaughlin B M and Bell K L 1998 *J. Phys.* B **31** 4317

[17] Aglitskii E V, Ivanova E P and Vainshtein L A 1989 *Phys. Scr.* **40** 601

[18] Dyall K G, Grant I P, Johnson C T, Parpia F A and Plummer E P 1989 *Comput. Phys. Commun.* **55** 425

[19] Temkin A 1957 *Phys. Rev.* A **107** 1004

[20] Au C K, Poon K L and Young K 1991 *J. Phys.* B **24** 4671

[21] Kaufman V and Sugar J 1986 *J. Phys. Chem. Ref. Data* **15** 321